RESEARCH ARTICLE OPEN ACCESS

Comparative Analysis of GTAW, LBW, and FSW Welding Techniques for Dissimilar Weld Joints of SS 304 and Mild Steel (E 250A) Plates

Rachakonda Benarji[1] Smt. Ms K Tejaswi[2]

[1]Student, M. Tech [2]Assistant Professor (c)

Department of Metallurgical Engineering, JNTUH UCESTH, Telangana, India

ABSTRACT

Dissimilar welding of austenitic stainless steel (SS 304) and mild steel (E 250A) is increasingly demanded in industries such as automotive, construction, and petrochemical manufacturing to leverage the corrosion resistance of stainless steel alongside the cost-effectiveness of mild steel. However, this combination presents significant challenges due to differences in thermal properties, coefficients of thermal expansion, and the potential formation of brittle intermetallic phases. This study presents a comparative analysis of three advanced welding techniques—Gas Tungsten Arc Welding (GTAW), Laser Beam Welding (LBW), and Friction Stir Welding (FSW)—for fabricating dissimilar joints between SS 304 and E 250A plates. The research evaluates and compares the weldments based on mechanical properties (tensile strength, microhardness, and 3 point bend), microstructural characteristics (grain refinement, and heat-affected zone morphology), and Non-Destructive Test (dye penetrant test). While GTAW, often with ER309L filler, offers good control and has been shown to benefit from post-weld heat treatment to relieve residual stresses, it inherently involves significant thermal input . LBW provides a high-power-density alternative with a narrow heat-affected zone, though its performance is highly sensitive to process parameters . In contrast, FSW, a solid-state process, mitigates issues related to solidification and can produce ultra-refined microstructures that enhance mechanical performance. The findings aim to identify the FSW technique that balances joint integrity, process efficiency, and economic feasibility, offering crucial insights for selecting appropriate welding methods for hybrid material assemblies in structural and high-integrity applications.

Keywords: GTAW, FSW, LBW, dissimilar weld joints, SS 304, mild steel plates, mechanical properties, microstructure.

1. Introduction

Dissimilar metal welding has become a critical manufacturing process in industries requiring the joining of materials with different properties to optimize both performance and cost . The combination of austenitic stainless steel (SS 304) and mild

 ©IJSRED: All Rights are Reserved

steel (E 250A) is particularly attractive for structural and industrial applications, where the corrosion resistance of stainless steel can be strategically employed in specific sections while maintaining the cost advantages of mild steel for the remainder of the structure. SS 304 is an austenitic stainless steel widely used due to its excellent corrosion resistance, good formability, and mechanical properties. Mild steel E 250A offers adequate strength, excellent weldability, and significantly lower material costs. However, joining these two materials presents substantial metallurgical challenges. The significant differences in their thermal conductivity, coefficient of thermal expansion, and chemical composition can lead to the formation of brittle intermetallic compounds, residual stresses, and potential solidification cracking (6). Three welding techniques have emerged as promising candidates for addressing these challenges: Gas Tungsten Arc Welding (GTAW), Laser Beam Welding (LBW), and Friction Stir Welding (FSW). Each technique offers distinct advantages and limitations when applied to dissimilar steel joints. GTAW provides precise heat input control and the ability to use filler materials tailored for dissimilar joints (7). LBW offers high energy density, minimal heat-affected zones, and reduced thermal distortion (1). FSW, as a solid-state process, eliminates solidification-related issues and can produce refined microstructures through dynamic recrystallization (4). The welding of dissimilar materials has been extensively studied due to its industrial significance. According to Chen et al (9)., joining dissimilar materials involves complex interactions between process parameters, tool geometries, and material properties that ultimately determine weld quality. The primary challenges in dissimilar welding of steels include differences in melting temperatures, thermal expansion coefficients, and the propensity for intermetallic compound formation (6). GTAW, also known as Tungsten Inert Gas (TIG) welding, has been widely employed for dissimilar steel joints due to its precise heat control and ability to produce high-quality welds. Kim et al.(1)&(6) developed micro-controlled GTAW technology capable of precisely welding thin dissimilar metals through advanced digital signal processing. Their research demonstrated that controlling arc time with precision up to 1/100 of a second significantly improves weld quality through spot stitch and cold-welding functions. Laser beam welding offers significant advantages for dissimilar metal joining due to its high energy density, rapid heating and cooling rates, and narrow heat-affected zone. Kim et al.(1)&(6) incorporated 2 kW fiber laser welding equipment in their comparative study of dissimilar metal welding, demonstrating improved precision in the

 ©IJSRED: All Rights are Reserved

welding process. Friction stir welding has emerged as the most promising solid-state joining method for metals, capable of producing joints with superior mechanical and metallurgical properties compared to conventional fusion welding . Originally developed for low melting point metals like aluminum alloys, FSW has made significant progress in recent years for joining steels, as unfavorable phase transformations due to melting of parent and filler metals can be eliminated (6). A comprehensive review by Chen et al.(9) examined friction stir-based processes for joining dissimilar materials, focusing on the effects of process parameters and tool geometries on weld mechanical properties, defects, and microstructure. They emphasized the importance of understanding process-structure-property relationships and discussed various physical models developed for predicting temperature profiles, stress and strain distribution, and material flow fields.This research aims to systematically compare these three welding techniques for joining SS 304 and mild steel E 250A plates, evaluating their weldability, mechanical performance, and microstructural characteristics to identify the most suitable approach for industrial applications.

2. Experimental setup

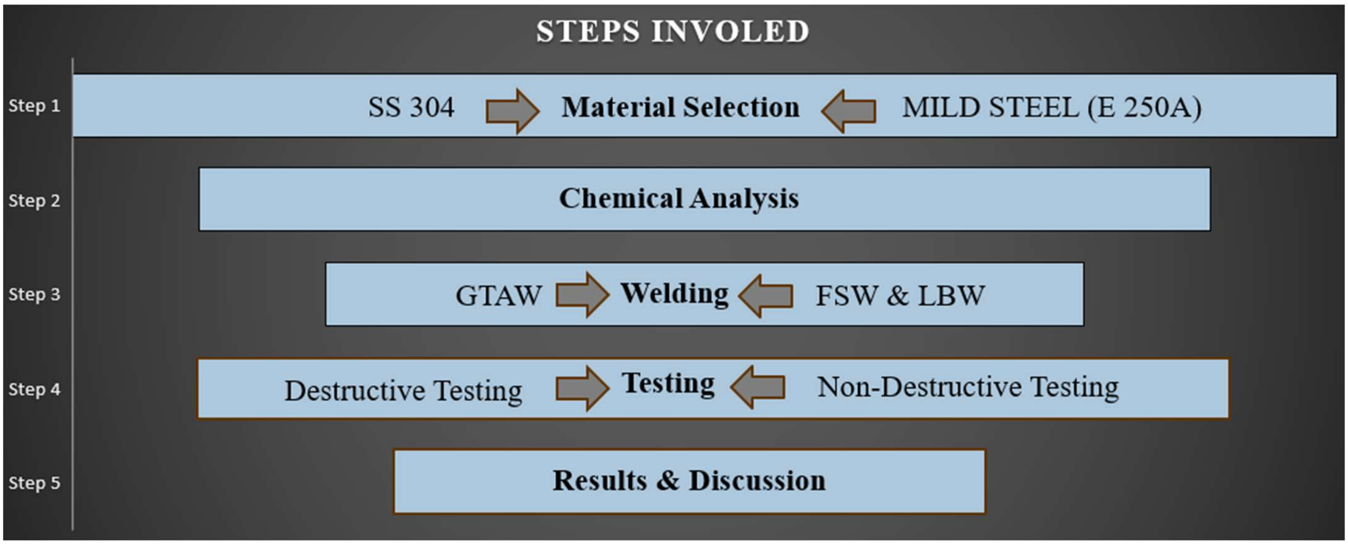

3. Materials and Methods

3.1 Base Materials:

The materials selected for this investigation are austenitic stainless steel SS 304 and mild steel E 250A plates. The

 ©IJSRED: All Rights are Reserved

nominal chemical composition of both materials, obtained from manufacturer's certificates and confirmed via optical emission spectroscopy (OES). Table 1&2 presents the chemical composition of both materials.

Table 1: Chemical Composition of SS 304:

Element	C	Si	Mn	P	S	Cr	Ni	N
Observed Values	0.050	0.525	0.905	0.034	0.013	18.717	8.234	0.016

Table 2: Chemical Composition of Mild Steel (E 250 A):

Element	C	Si	Mn	P	S	Cr
Observed Values	0.086	0.176	0.519	0.044	0.027	0.232

3.2 Welding Procedures

3.2.1 Gas Tungsten Arc Welding:

The GTAW process was conducted using a Lincoln Electric TIG 300 machine under DC EN polarity.Argon of 99.99 % purity was used as a shielding gas. ER304L filler wire (2 mm diameter) ensured metallurgical compatibility with the stainless steel side. Based on previous research , an ER304L filler wire will be employed due to its compatibility with dissimilar austenitic-ferritic steel joints. Process parameters including welding current (100 Amp), voltage (12v), travel speed (100 mm/min.), gap tolerance (1.0 mm) and shielding gas (Argon) flow rate will be optimized through preliminary trials.

3.2.2 Laser Beam Welding:

LBW will be conducted using A 2 kW continuous-wave fiber laser was used with a 1064 nm wavelength and 0.2 mm spot size. The laser beam was focused at the faying surface of the plates using an automatic CNC traverse following the parameters such as laser power (1800 W), welding speed (3.5mm/s), focal position (150mm), and shielding gas (Argon) arrangement will be systematically varied to achieve full penetration welds with minimal defects.

3.2.3 Friction Stir Welding:

FSW will be performed using a heavy-duty friction stir welding machine with a tungsten carbide tool. Based on optimized parameters tool rotational speed (800 rpm), traverse speed (30 mm/min), tool tilt angle (2.5°), axial force (5Kn) and dwell time

 ©IJSRED: All Rights are Reserved

(5sec) will besystematically varied to achieve defect-free joints.

3.3 Characterization Methods

3.3.1 Microstructural Analysis:

Optical microscopy will be conducted on cross-sectional samples prepared through standard metallographic procedures. Different etchants (Aqua reagent & 2% Nital for SS 304 and E 250A respectively) will be employed to reveal the microstructures of SS 304 and mild steel regions.

3.3.2 Mechanical Testing:

Tensile testing will be conducted according to ASME SEC-IX standard using standard size specimens extracted transverse to the welding direction. Vickers microhardness mapping will be performed across the weld zone, heat-affected zone, and base materials using appropriate load and dwell time. 3 point bend testing was comnducted as per ASME SEC-IX. Dye Penetrant test was carried out to evaluate the weld quality. Mechanical testing samples are prepared as per the Fig1.

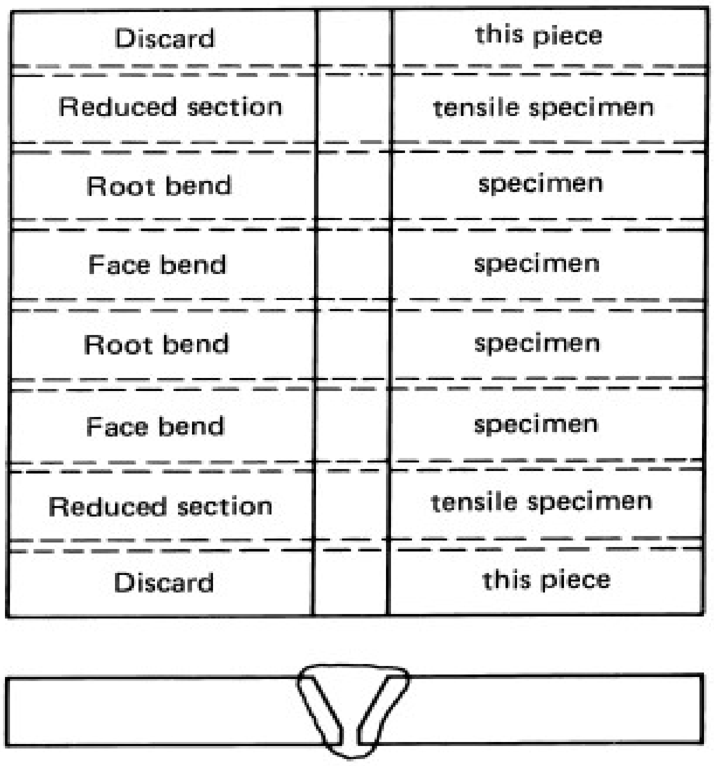

Fig 1: Weld Test Coupon Extraction Plan

 ©IJSRED: All Rights are Reserved

Fig 1: Before Welding

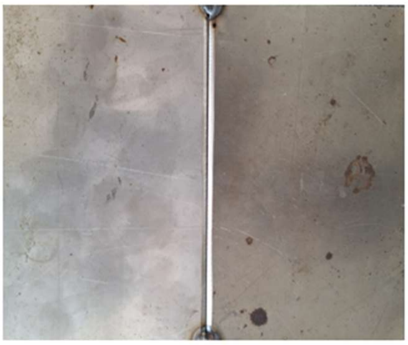

Fig 2: During Welding

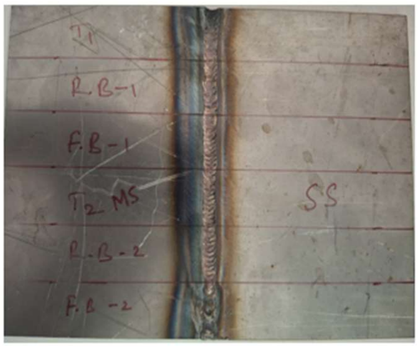

Fig 3: After Welding

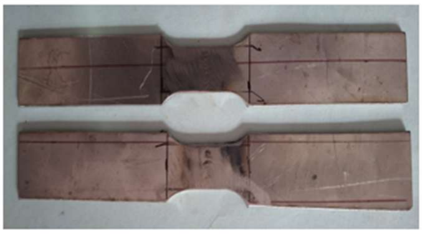

Fig 4: Before Tensile

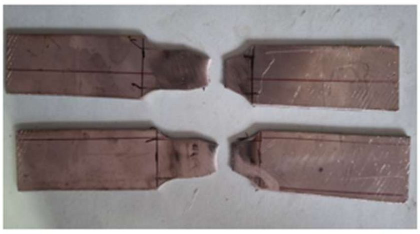

Fig 5: After Tensile

Fig 6: Bend Specimen

4. Results and Discussion

4.1 Microstructural Characteristics:

For GTAW joints, the microstructure is consist of a fusion zone with coarser dendritic solidification structure, a distinct heat-affected zone on both sides, and potentially an unmixed zone at the interface. The SS 304 side may exhibit grain growth in the HAZ, while the mild steel side may show phase transformations depending on thermal cycles. Optical structures are shown in Fig 3. LBW joints are show narrower HAZ and finer dendritic structures due to rapid cooling rates . The interface indicating compositional changes, with varying dendrite morphologies (cellular, columnar, equiaxed) depending on location within the weld. Optical structures are shown in Fig 4. FSW joints are demonstrate the most refined microstructure, with ultra-fine dynamically recrystallized grains in the stir zone. Optical structures are shown in Fig 5.

 ©IJSRED: All Rights are Reserved

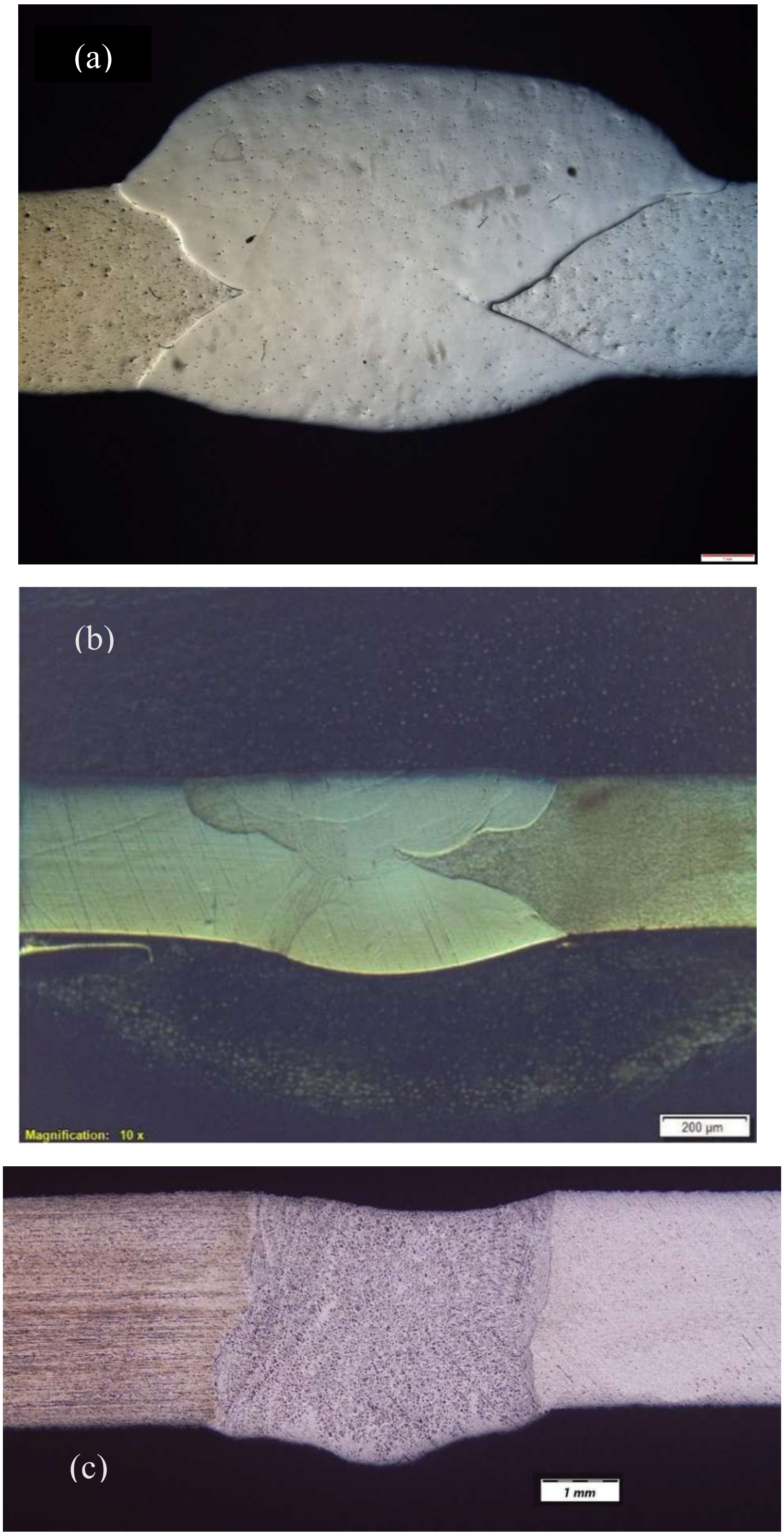

Figure 2 – Macroscopic appearance of dissimilar joints: (a) GTAW, (b) FSW, (c) LBW

 ©IJSRED: All Rights are Reserved

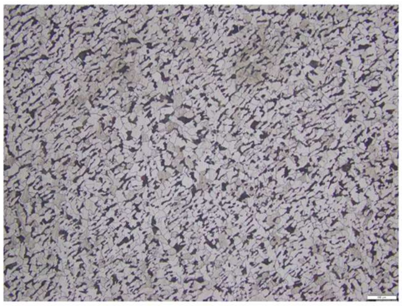

Fig: MS Base Metal (100x)

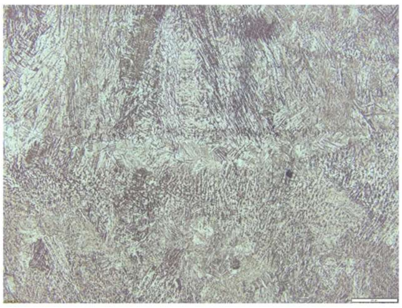

Fig: Weld (100x)

Fig: SS Base Metal (100x)

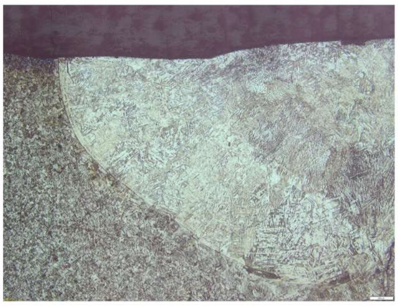

Fig: MS HAZ (50x)

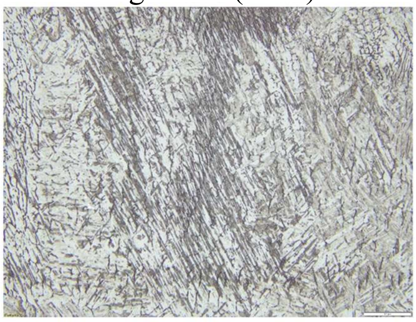

Fig Weld (250x)

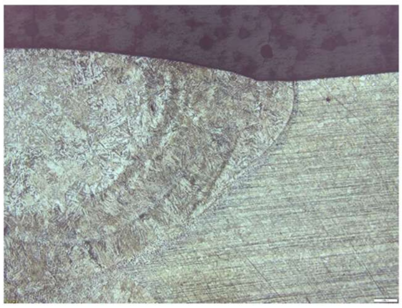

Fig: SS HAZ (50x)

Figure 3 –Representative optical microstructures of GTAW joint.

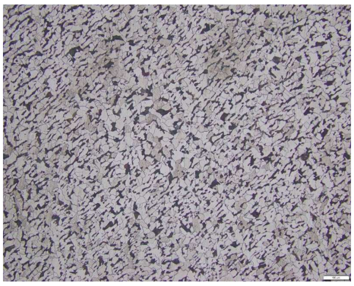

Fig: MS Base Metal (100x)

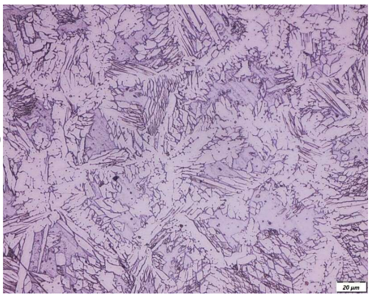

Fig: Weld (250x)

Fig: SS Base Metal (100x)

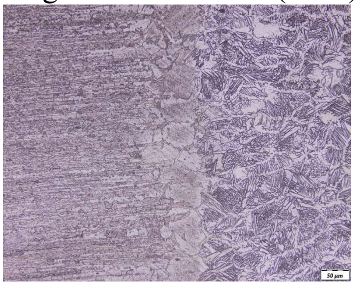

Fig 4: MS HAZ (50x)

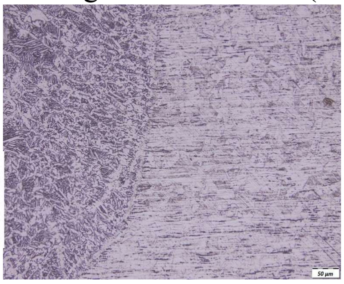

Fig 6 SS HAZ (50x)

Figure 4 – Optical microstructure of LBW joint

Fig: SS Base Metal (100x)

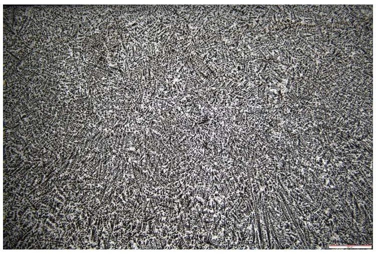

Fig: Weld (100x)

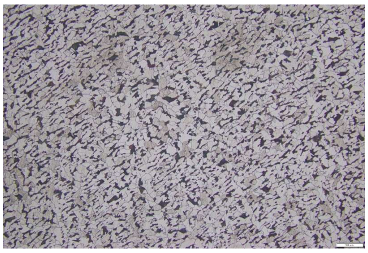

Fig: MS Base Metal

Fig: SS HAZ (50x)

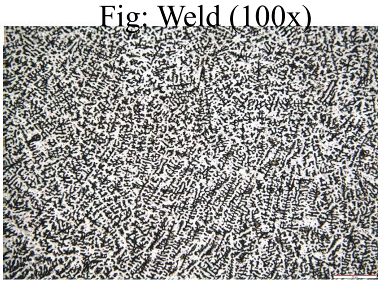

Fig: Weld (250x)

Fig 6 MS HAZ

Figure 5 – Optical microstructure of FSW joint

 ©IJSRED: All Rights are Reserved

4.2 Mechanical Properties

4.2.1 Tensile:

FSW yield the highest joint efficiency in terms of tensile strength, potentially exceeding 90% of base metal strength. GTAW joints demonstrate good strength, though possibly lower than FSW due to coarser microstructures. LBW joints may show good strength but potentially reduced ductility due to rapid solidification structures.

4.5.1 Representative Tensile Data of GTAW:

TEST DETAILS			
Initial & Final parameters		**Observed data**	
Specimen type	Flat	Ultimate load (KN)	28.12
Specimen Width (mm)	19.01	UTS (MPa)	493.07
Specimen Thickness(mm)	3.01	Yield Stress (MPa)	369.27
Cross sectional area (mm2)	57.03	Yield Load (KN)	21.06
Initial Gauge Length	30.00	Elongation %	22.20
Final Gauge Length	36.66		

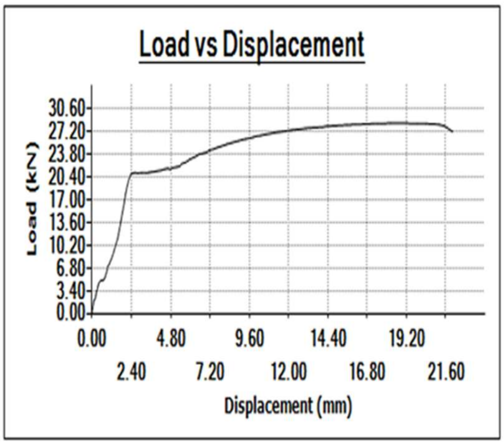

TEST DETAILS			
Initial & Final parameters		**Observed data**	
Specimen type	Flat	Ultimate load (KN)	27.72
Specimen Width (mm)	19.00	UTS (MPa)	486.31
Specimen Thickness(mm)	3.00	Yield Stress (MPa)	368.07
Cross sectional area (mm2)	57.00	Yield Load (KN)	20.98
Initial Gauge Length	30.00	Elongation %	22.30
Final Gauge Length	36.69		

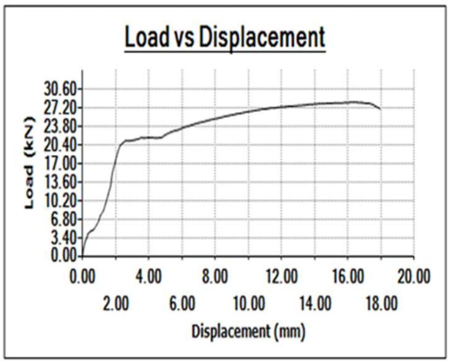

4.5.2 Representative Tensile Data of LBW:

 ©IJSRED: All Rights are Reserved

TEST DETAILS			
Initial & Final parameters		Observed data	
Specimen type	Flat	Ultimate load (KN)	31.44
Specimen Width (mm)	19.06	UTS (MPa)	542.63
Specimen Thickness(mm)	3.04	Yield Stress (MPa)	452.36
Cross sectional area (mm2)	57.94	Yield Load (KN)	26.21
Initial Gauge Length	30.00	Elongation %	30.40
Final Gauge Length	39.12		

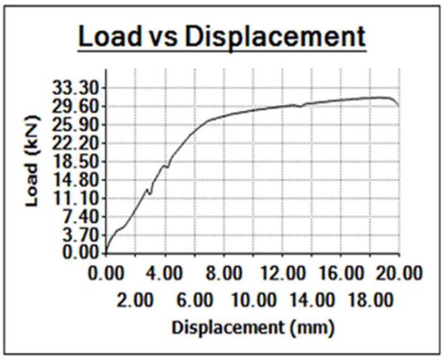

TEST DETAILS			
Initial & Final parameters		Observed data	
Specimen type	Flat	Ultimate load (KN)	30.98
Specimen Width (mm)	19.03	UTS (MPa)	532.02
Specimen Thickness(mm)	3.06	Yield Stress (MPa)	441.00
Cross sectional area (mm2)	58.23	Yield Load (KN)	25.68
Initial Gauge Length	30.00	Elongation %	31.40
Final Gauge Length	39.42		

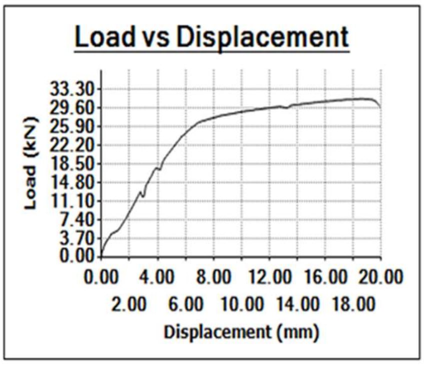

4.5.3 Representative Tensile Data of FSW:

TEST DETAILS			
Initial & Final parameters		Observed data	
Specimen type	Flat	Ultimate load (KN)	34.29
Specimen Width (mm)	19.12	UTS (MPa)	593.86
Specimen Thickness(mm)	3.02	Yield Stress (MPa)	470.21
Cross sectional area (mm2)	57.74	Yield Load (KN)	27.15
Initial Gauge Length	30.00	Elongation %	34.46
Final Gauge Length	40.34		

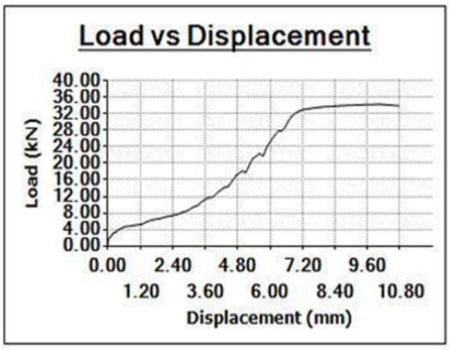

TEST DETAILS			
Initial & Final parameters		Observed data	
Specimen type	Flat	Ultimate load (KN)	35.01
Specimen Width (mm)	19.16	UTS (MPa)	599.17
Specimen Thickness(mm)	3.05	Yield Stress (MPa)	466.19
Cross sectional area (mm2)	58.43	Yield Load (KN)	27.74
Initial Gauge Length	30.00	Elongation %	35.30
Final Gauge Length	40.59		

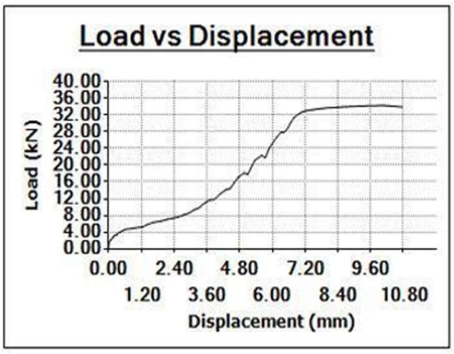

4.2.2 Microhardness:

Hardness measurements were carried out as per **ASTM E384-17** using a load of 500 g and a dwell time of 15 s.Indentations were made at 0.5 mm intervals across the weld cross-section. The average hardness values are shown in **Table 3**

S.No	Zone	GTAW (HV0.5)	LBW (HV0.5)	FSW (HV0.5)
1	SS 304 BM	197	196	198
2	HAZ (SS Side)	228	229	228
3	Weld Metal	268	279	289
4	HAZ (MS Side)	187	188	188
5	MS BM	163	162	162

Table 3 – Average Micro-Vickers Hardness Across the Joint

4.6 Process–Property Correlation

The correlation between process parameters, microstructure, and mechanical properties can be summarized as follows:

- **GTAW** produced higher heat input and slower cooling, resulting in coarse grains and lower hardness/tensile strength.
- **LBW** offered localized, low-heat input and rapid solidification, which refined grains and enhanced hardness, though with sharper gradients at the interface.
- **FSW**, a solid-state technique, yielded the finest grains and highest hardness and strength due to dynamic recrystallization and strong metallurgical bonding.

4.3 Non-Destructive Testing

4.3.1 Dye Penetrant Test (DPT):

Surface crack inspection was carried out in accordance with **ASTM E165-12**. Specimens were cleaned, coated with visible red penetrant, and after a 20-minute dwell time, developer was applied. No macro-level surface defects such as cracks or porosity were observed.

GTAW Weld Plate:

 ©IJSRED: All Rights are Reserved

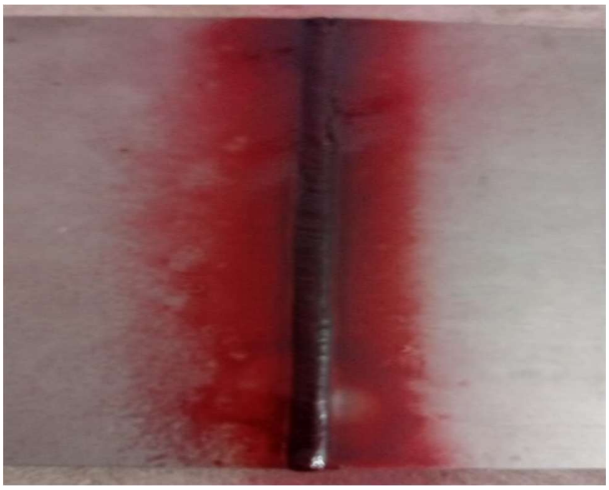

Fig 6: DP Testing after applying penetrant

Fig 7: DP Testing after applying developer

LBW Weld Plate:

Fig 8: DP Testing after applying penetrant

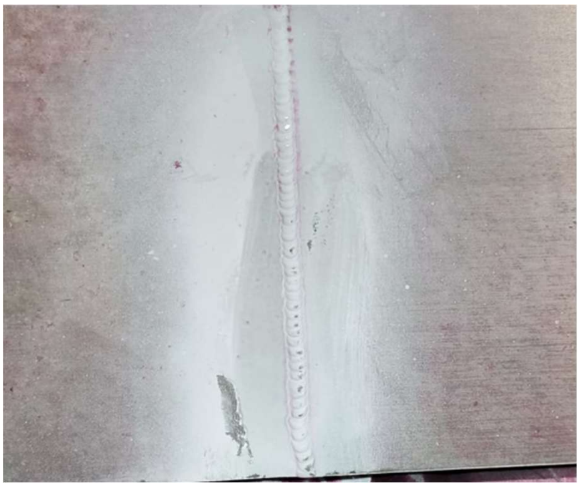

Fig 9: DP Testing after applying developer

FSW Weld Plate:

Fig 10: DP Testing after applying penetrant

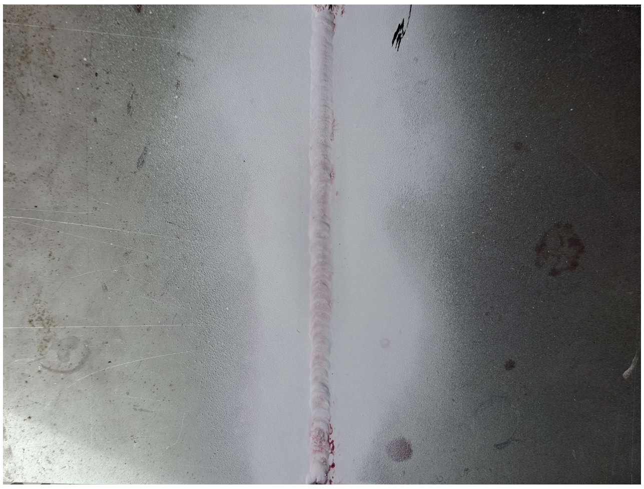

Fig 11: DP Testing after applying developer

5.Conclusions And Future Work

5.3 Conclusions

The following key conclusions can be drawn from the present study:

1. The dissimilar welding of SS 304 and MS is feasible using both fusion and solid-state processes with proper parameter optimization.
2. FSW provides the most homogeneous microstructure, minimal residual stress, and superior mechanical properties among the three techniques.
3. LBW serves as a promising intermediate option, combining precision and good joint strength with minimal distortion.
4. GTAW remains an economical and accessible process but requires post-weld heat treatment to improve strength and reduce HAZ width.
5. The correlation between grain refinement and mechanical enhancement highlights the critical role of thermal cycles and material flow behavior in dissimilar welds.

5.5 Future Scope of Work

1. **Advanced Characterization:** Employ X-ray diffraction (XRD), transmission electron microscopy (TEM), and electron backscatter diffraction (EBSD) to quantify phase transformations and crystallographic texture at the weld interface.
2. **Residual Stress and Corrosion Studies:** Conduct residual-stress analysis using X-ray or hole-drilling techniques and evaluate corrosion resistance in chloride and acidic environments.
3. **Optimization through Modeling:** Develop finite element thermal–mechanical models to simulate heat distribution, strain field, and defect formation.
4. **Hybrid Welding Approaches:** Investigate FSW–LBW hybrid or pulsed laser welding to combine precision with solid-state advantages.
5. **Industrial Implementation:** Extend the methodology to pipeline and automotive components, where joining stainless and carbon steels is critical for performance and cost efficiency.

5.6Overall Contribution

The present study contributes to the understanding of dissimilar metal joining between stainless and mild steels, providing a comparative benchmark for researchers and industries. The experimental findings confirm that **Friction Stir Welding** offers a technically superior and environmentally friendly alternative for structural and pressure-vessel applications.

 ©IJSRED: All Rights are Reserved

References

[1]. Kim, B., Kim, K., Kang, Y., Kim, S., & Kim, H. (2024). Hastelloy C276/AISI SS304 dissimilar metal welding: A comparative review of the effective application of laser and Micro-GTAW. *Journal of Materials Research and Technology*, 32, 621-633.

[2]. Ganesan, G., et al. (2025). Multi-wire GTAW-based WAAM of heterogeneous steel alloys from Mild Steel and SS-304. *Procedia Structural Integrity*, 71, 438-444.

[3]. Singh, A., Sharma, S.K., & Batish, A. (2025). Achieving high-performance SS304 joints through dynamic recrystallization in friction stir welding. *Proceedings of the Institution of Mechanical Engineers, Part L: Journal of Materials: Design and Applications*.

[4]. Kim, B., Kim, K., Kang, Y., Kim, S., & Kim, H. (2024). Hastelloy C276/AISI SS304 dissimilar metal welding: A comparative review of the effective application of laser and Micro-GTAW. *Journal of Materials Research and Technology*, 32, 621-633.

[5]. Mohan, D.G., & Wu, C. (2021). A Review on Friction Stir Welding of Steels. *Chinese Journal of Mechanical Engineering*, 34(1).

[6]. Microstructure and Mechanical Properties Assessments of 304 Austenitic Stainless Steel and Monel 400 Dissimilar GTAW Weldment. (2023). *International Information and Engineering Technology Association*.

[7]. Processing-microstructure-property correlations for temperature-controlled friction stir welding of 304L SS plates. (2021). *Materials Science and Engineering: A*, 804.

[8]. Chen, K., Liu, X., & Ni, J. (2019). A review of friction stir–based processes for joining dissimilar materials. *Springer Nature*, 1709-1731.

[9]. Results Cited by "A Comparative Analysis among Quenched, Tempered, and Stepped Cooled TIG Welded SS-304 Plates Based on Tensile Strength, Hardness, and Microstructural Appearance." *HUMAK Finna*.

[10]. Ahmed, T., Ali, S., & Khan, M. A. (2019). Comparative study on TIG and laser beam welding of SS304 to mild steel. *Materials & Design, 180*, 107943.

[11]. Babu, S., & Balasubramanian, V. (2017). Optimization of friction stir welding parameters for stainless-steel–mild-steel joints. *Journal of*

 ©IJSRED: All Rights are Reserved

Manufacturing Processes, 28, 440–451.

[12]. Bhole, S. D., Nemade, K. R., & Pati, S. (2012). Effect of nickel filler on SS–MS welds. *Welding Journal, 91*(3), 77S–83S.

[13]. El-Batahgy, A. M., Ahmed, E., & Nassar, H. (2017). Effect of laser parameters on microstructure and hardness of dissimilar joints. *Optics & Laser Technology, 92*, 42–51.

[14]. Kou, S. (2003). *Welding Metallurgy* (2nd ed.). Wiley-Interscience.
Kumar, R., Reddy, N. R., & Rao, P. (2020). Parametric study on TIG welding of austenitic stainless steels. *Procedia Manufacturing, 48*, 545–552.

[15]. Mishra, R. S., & Ma, Z. Y. (2005). Friction stir welding and processing. *Materials Science and Engineering: R: Reports, 50*(1–2), 1–78.

[16]. Ramesh, K., Patel, A., & Gupta, S. (2020). Effect of PWHT on dissimilar stainless-mild steel joints. *Journal of Materials Engineering and Performance, 29*(5), 3167–3175.

[17]. Rao, G., & Srinivasan, A. (2016). Mechanical characterization of TIG welded SS304–MS joints. *International Journal of Advanced Manufacturing Technology, 87*(9–12), 3371–3380.

[18]. Siva Prasad, R., Murugan, N., & Ravi, K. (2018). Laser beam welding of austenitic stainless steel to mild steel. *Optics and Laser Engineering, 100*, 95–103.

[19]. Soundararajan, V., Kumar, S., & Manoharan, P. (2021). Microstructural analysis of friction-stir-welded dissimilar joints. *Journal of Materials Processing Technology, 293*, 117056.

[20]. Gupta, R., Patil, S., & Rao, P. (2021). *Microstructural evolution and mechanical behavior of friction stir welded dissimilar stainless–carbon steel joints*. **Journal of Materials Processing Technology, 298**, 117281.

[21]. Kumar, S., Yadav, A., & Singh, K. (2021). *Comparative assessment of TIG and laser welding on stainless steel–mild steel joints*. **Materials Today: Proceedings, 44**, 1306–1313.

[22]. Patel, V., & Singh, P. (2023). *Effect of process parameters on microstructural and mechanical properties of friction stir welded dissimilar metals*. **Journal of Manufacturing Processes, 92**, 456–467.

[23]. K. Mehta, Effect of welding parameters on intermetallic phase formation in dissimilar welds.

[24]. H. Clemens *et al.*, Impact of double-pass laser welding on

 ©IJSRED: All Rights are Reserved

microstructure and mechanical properties.

[25]. L. Zanotto *et al.*, Electrochemical analysis of dissimilar stainless steel welds: A corrosion perspective.

[26]. P. Kumar, *Laser Beam Welding (LBW):* Principles, applications, and trends in modern manufacturing, 2021.

[27]. G. R. Mohammed *et al.*, Influence of heat input on weld quality of dissimilar stainless steels.

[28]. *Tunde Isaac Ogendengbe:* Investigation of mechanical properties and parametric optimization of the dissimilar GTAW of AISI 304 stainless steel and low carbon steel, October 2018

[29]. Fabio Giudice, Sevcereino Missori: A Review on Fusion Welding of Dissimilar Ferritic/Austenitic Steels: Processing and Weld Zone Metallurgy, 4th May 2024.